Project Summary

Dynamics and Forcing of Nares Strait from 2003-09: Tidal to Interannual Variability to the West of Greenland

Andreas Münchow and Helga S. Huntley

Intellectual Merit This proposal seeks support to test the hypothesis that the dynamics of Nares Strait is in a state of transition as the season of landfast ice cover diminishes. To do so, we propose to analyze a comprehensive 6-year data set from an array of moored ocean current, salinity, temperature, sea level, and subsurface pressure sensors, as well as ice thickness observations. The data originate from an unprecedented, high-risk, but ultimately successful 2003-2009 Canada-US observational program that took place in Nares Strait, a major pathway of Arctic waters into the North Atlantic to the west of Greenland. We propose to describe and explain the temporally and spatially varying regimes of kinematics and dynamics within this energetic channel. As oceanic fields are forced by vertical and horizontal boundary layer physics at the ice-water, air-water, and ice-air interfaces, the program includes synthesis of data from a meteorological modeling, a remotely-sensed ice (MODIS), and an ice modeling (CICE) component.

The moored array was deployed in 2003, serviced in 2006 and 2007, and finally recovered in 2009. Münchow and Melling (2008) and Rabe et al. (2010) present first results on the depth-averaged ocean currents and vertical stratification of salinity and temperature, respectively, for the 2003-06 period. The second 2007-09 deployment resulted in a complete record as all instruments were recovered without any gaps. These data allow us to test the hypothesis that the freshwater flux through the Canadian Archipelago presently transitions from a dynamic state that is characterized by land-fast ice to one that is characterized by mobile ice. This regime change causes more variable ice and ocean motion as well as potential increase in freshwater flux by 50%, because the system responds more strongly to time-dependent local atmospheric forcing in addition to remote forcing. Temporal variations of ocean stratification and freshwater flux take place at spatial scales that include fundamental geophysical scales for fluids under the influence of rotation (Rossby radius of deformation), geometric scales set by topography, and scales related to vertical and lateral boundary layer processes such as friction.

Broader Impacts The proposed effort will support first-year Ph.D students Patricia Ryan and Jamie Shutta in addition to two undergraduate and two local science teachers as summer interns with the PIs facilitating daily workshops. The education of students and teachers to critically evaluate physical and statistical methods, data, and analyses is needed to improve both public and scientific debate related to climate change. This proposal contributes substantially to US participation, continuity, and data dissemination within an ongoing, informal, international, collaborative effort of a "Friends of Nares Strait" group that includes young and old researchers from Denmark, Scotland, England, Canada, and the USA. Canadian, Danish, and US government agencies and private service providers frequently rely on our data and expertise in order to aid their clients, e.g. with oil exploration, icebreaking operations, or natural resource management.

TABLE OF CONTENTS

For font size and page formatting specifications, see GPG section II.B.2.

*Proposers may select any numbering mechanism for the proposal. The entire proposal however, must be paginated. Complete both columns only if the proposal is numbered consecutively.

Results from Prior NSF Support

"Collaborative Research: Variability and Forcing of Fluxes through Nares Strait and Jones Sound" *OPP-0230236* (Münchow and Wong); 1/1/2003-12/31/2007 , $2,052,911

This 5-year effort with Oregon State University (Dr. Falkner) and the Institute of Ocean Sciences, Canada (Dr. Melling) provided moored and survey data from Nares Strait (Figure 1A) to estimate fluxes via the Canadian Archipelago into the North Atlantic to the west of northern Greenland as part of the Arctic-Subarctic-Ocean-Flux (ASOF) experiment. Our web-site http://www.udel.edu/CATS contains processed data, reports, peer-reviewed papers, and outreach materials. In 2003 we deployed 17 moorings to measure ocean current, salinity, and temperature profiles as well as subsurface pressure and ice thickness from the USCGC Healy. In 2006, 15 moorings were recovered with complete and gap-free 3-year data records (Münchow and Melling, 2008; Rabe et al., 2010). We discuss selected findings below as they relate to the present analysis proposal.

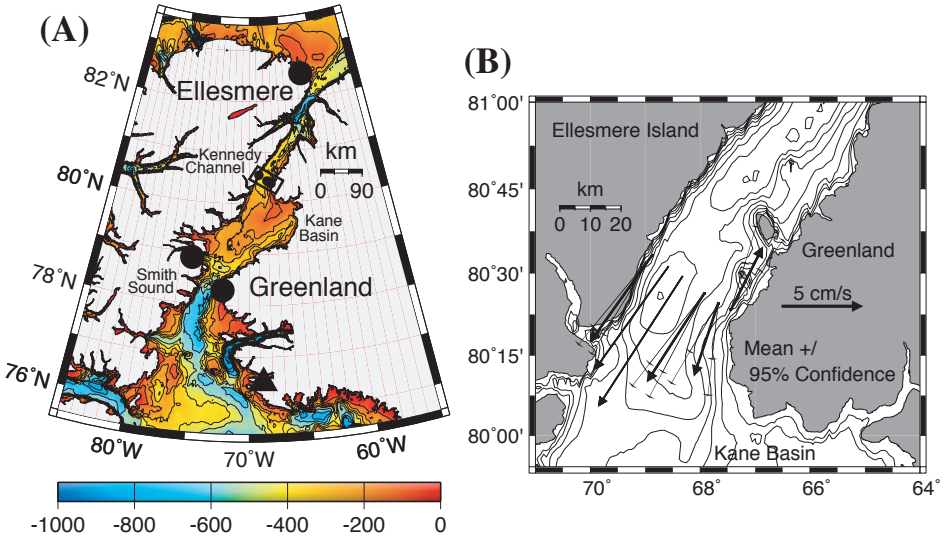

Figure 1: (A) Map of the study area with 2003-06 instrument locations. Triangle indicates Thule (Greenland); circles indicate locations of bottom pressure meters at Foulke (Greenland) and Alexandra (Ellesmere Island) Fjords, and a tide gauge at Alert (Ellesmere Island). Subsurface mooring locations of 4 ADCPs are indicated by small circles inside the polygon at 80.5N latitude; additional 6 temperature-salinity moorings with 4 instruments each on this section are not shown. Contours are bottom depth in 100 m increments. (B) Record-mean vertically averaged flow for 2003-06 with 95% confidence limits. Thin vectors without confidence limits represent interpolated flow (Münchow and Melling, 2008). The contours are isobaths in 50-m intervals.

The Healy vessel-mounted acoustic Doppler current profiler (ADCP) revealed unexpectedly rich ocean currents after we processed the data with a newly designed algorithm. Results indicated that both barotropic (1/3) and baroclinic (2/3) processes contribute to volume, and freshwater flux (Münchow et al., 2006). Combining tracer with velocity observations, we demonstrated that Pacific water contributes to the throughflow at Nares

Strait contrary to previous assertions (Münchow et al., 2007; Falkner et al., 2009).

Samelson et al. (2006) report on the interaction of strong ageostrophic atmospheric motion in Nares Strait and the formation of ice-arches anchored to the coasts of both Greenland and Canada whose formation is impacted by strong tidal currents.

The project supported three undergraduate summer intern and three graduate students. Ms. Zweng completed an MS degree reporting on significant warming and freshening trends in Baffin Bay and along Baffin Island, respectively, for the 1916-2003 period (Zweng and Münchow, 2006). Ms. Brown was an undergraduate intern in 2003 who is in the final stages of completion of an MS thesis on Nares Strait hydrography. Ph.D student Ms. Rabe submitted Rabe et al. (2010) on the analysis of the 2003-06 data set. She will defend her dissertation in the spring of 2010.

PROJECT DESCRIPTION

1 Introduction

The Canadian Archipelago and Fram Strait constitute the two pathways for the exchange of water and ice between the Arctic and Atlantic Oceans. Arctic outflows via these pathways return freshwater to the North Atlantic that was evaporated from tropical oceans, transported by the atmosphere, and delivered to the Arctic Ocean via precipitation, terrestrial run-off, and inflow from the North Pacific (Emile-Geay et al., 2003). We here focus on through-flows west of Greenland via Nares Strait which is a major conduit of southward flux into Baffin Bay and the Atlantic Ocean. Fluxes through Nares Strait reflect the impacts of diminishing sea ice in the Arctic (Parkinson and Cavalieri, 2008), disintegrating ice shelves of northern Canada (Copland et al., 2007), and potentially surging glaciers of northern Greenland (Rignot and Steffen, 2008).

From a hydrologic perspective, the pack ice and upper few hundred meters of the Arctic Ocean are a reservoir of nearly 100,000 km^3 of freshwater (Aagaard and Carmack, 1989; Proshutinsky et al., 2009). Because this is about 15 times larger than the annual input, the Arctic Ocean buffers imbalances in its freshwater budget. Conversely, the reservoir has the capacity to deliver large pulses of freshwater to the Atlantic. The factors influencing storage and release are poorly understood, but substantial change has been demonstrated such as a shift in the boundary between Atlantic- and Pacific-derived waters (Morison et al., 1998); a shift in the position of the trans-polar drift (Rigor et al., 2002); retreat and return of the cold halocline in the Eurasian Basin (Alkire et al., 2007); reduced pack ice (Lindsay et al., 2009); changes in freshwater content (Polyakov et al., 2008); increased run-off into the Eurasian sector (Peterson et al., 2002); and many more (White et al., 2007). Most changes appear to correlate with atmospheric forcing (Serreze and Francis, 2006).

Meanwhile, impacts of variable freshwater export occurring downstream of the Arctic have been observed in the formation zones for North Atlantic deep waters in the Green-

land and Labrador Seas such as the Great Salinity Anomaly spreading over the North Atlantic since 1970 (Belkin, 2004) and a more recent freshening of deep waters both in the North-Atlantic (Curry and Mauritzen, 2005) and adjacent isolated basins such as Baffin Bay (Zweng and Münchow, 2006). Models and observations link the propagation of these signals to atmospheric variations (Sundby and Drinkwater, 2007; Hurrell and Deser, 2009). Furthermore, models predict that increased surface freshening and warming in the Greenland and Labrador Seas will slow global overturning of the oceans (Koenigk et al., 2007). Possible early evidence for such slowing has been recently reported (Bryden et al., 2005), although Wunsch and Heimbach (2006) suggests that aliasing may explain some of the observed trends in hydrographic observations.

The cold fresh Arctic outflows from Nares Strait and Lancaster Sound become the Baffin Island Current that flows southward through the Davis Strait and contributes substantially to the fresh shelf and slope waters off Labrador (Khatiwala et al., 1999). Numerical global climate scenarios appear sensitive to the parameterization of both the physical processes and pathways of Arctic to sub-Arctic exchange of water (Curry and Mauritzen, 2005) and vorticity (Yang, 2005). More specifically, the presence of Arctic outflows both west and east of Greenland appears to improve model performance relative to those climate models without a Canadian Archipelago (Holland et al., 2007).

Efforts to compile estimates of various component fluxes through the Arctic gateways have generally asserted that the freshwater fluxes east and west of Greenland are of more or less equal size. The most recent such effort (Dickson et al., 2007) realized, however, that the fluxes to the east and west of Greenland are (a) potentially unsteady and (b) impact the overturning circulation differently. More specifically, the impact of the Arctic freshwater outflow on the global overturning circulation depends on whether (a) it is spread to depth in the Atlantic Ocean via the overflow system from Nordic Seas, e.g. Denmark Strait to the east of Greenland (Dickson et al., 2002), (b) it is inserted is at the surface of the North-Atlantic, or (c) it is trapped on continental shelves (Khatiwala et al., 1999; Myers, 2005). Koenigk et al. (2007) predict a likely 48% increase in the freshwater flux through the Canadian Archipelago, compared to only a 3% increase through Fram Strait, as a result of a much diminished Arctic ice cover.

Direct measurements of flow within the Canadian Archipelago are sparse (Melling et al., 2008). Strong and persistent currents have been measured in Robeson channel (Sadler, 1976), in Smith Sound (Melling et al., 2001), and in Barrow Strait (Prinsenberg and Hamilton, 2005). Currents are strongest at the surface near the western side of channels (Münchow et al., 2007). Strong (30-300 cm/s) tidal currents in shallow water are a source of turbulent kinetic energy that reduces stratification through mixing and weakens the baroclinic component of flow. Covariance between velocity and salinity at tidal frequencies can contribute significantly to freshwater flux (Münchow et al., 2006). There are no in-situ data at present on freshwater flux by ice drift through the Archipelago.

2 Goals and Hypotheses

We propose to quantify properties and advective fluxes of the interacting components of the ice-ocean-atmosphere system at the relevant temporal and spatial scales in Nares Strait from 2003 to 2009. Temporal variations of ocean stratification and freshwater flux in Nares Strait take place at spatial scales that include (1) fundamental geophysical scales for fluids under the influence of rotation, (2) geometric scales set by topography, and (3) scales related to both vertical and lateral boundary layer processes such as friction. Changes in the duration of landfast ice conditions impact vertical and horizontal stratification as well as the distribution, transit times, and pathways of Arctic freshwater.

Our goal is to address two linked hypotheses concerning Arctic freshwater flux.

H1. Freshwater flux through the Canadian Archipelago presently transitions from a dynamic state characterized by land-fast ice (that we define as the winter regime) to one characterized by mobile ice (that we define as the summer regime).

H2. This regime change towards a longer mobile summer ice regime leads to more variable ice and ocean freshwater flux as the waters of Nares Strait become exposed to time-dependent local atmospheric surface forcing in addition to remote forcing by the ambient Arctic Ocean and Baffin Bay.

We emphasize that H1 and H2 are provisional ideas to be tested with analyses of moored and satellite observations along with idealized modeling of ice and channel flows. As oceanic fields are forced by boundary layer physics at the ice-water, air-water, and ice-air interfaces, our program includes synthesis of data from a meteorological modeling, a remotely-sensed ice, and an ice modeling component.

The hypotheses lead from descriptive to dynamical expositions of a complex channel flow where the ice, ocean, and atmosphere interact. These interactions range from tidal to decadal time scales with corresponding vertical and horizontal scales that reflect specific channel flow dynamics (Valle-Levinson, 2008; Johnson and Garrett, 2006; Garrett, 2004). The results, though focused on Nares Strait, have wider applicability within the Canadian Archipelago and mid-latitude channel flows (Stacey et al., 1991; Toulany et al., 1987).

3 Context

3.1 Observational Framework

This proposal aims to quantify spatial and temporal variability of fluxes through Nares Strait, a major passage of the Canadian Archipelago. From 2003 through 2009, a moored array measured ocean and ice properties from which fluxes can be estimated. Münchow and Melling (2008) discuss vertically averaged properties for the 2003-06 period using averaged velocity vectors, model wind predictions (Samelson and Babour, 2008), as well as observational estimates of along- and across-channel pressure gradients. Data from a

second deployment from 2007 through 2009 were retrieved in August of 2009.

Our 2003-06 data characterize an ice-ocean system where ice does not move for ∼6-9 months every year as a southern ice arch blocks ice advection (Dumont et al., 2009) resulting in a recurrent North Water polynya (Melling et al., 2001). This ice bridge in Smith Sound failed to form in 2006/07 (Münchow et al., 2007) and again in 2008/09. These first recorded failure may indicate a shift to a different dynamic regime. The new regime allows larger ice fluxes, an "earlier" open water season, and an extended period of thick ice streaming through Nares Strait. Less obvious, such conditions appear conducive to large increases in ocean freshwater flux. Figure 2 shows time series of geostrophic volume and freshwater fluxes, including conditionally averaged ocean flux sorted by winter (landfast ice) and summer (mobile ice) seasons. While volume flux appears similar in summer and winter, the summer freshwater flux is ∼50% larger than winter values. Since the conditions for the 2008/09 ice season represent a "year without a winter," we hypothesize much enhanced freshwater flux in 2009.

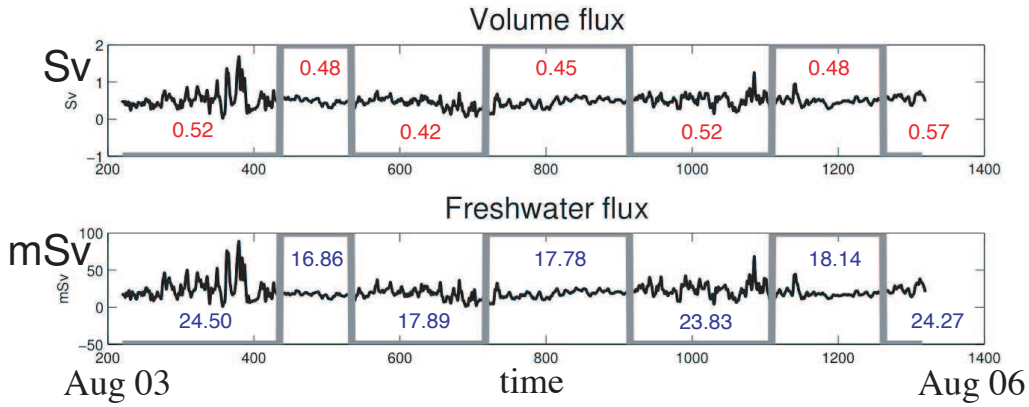

Figure 2: Timeseries of ocean volume and freshwater flux from 2003-06 observations assuming a geostrophic force balance. Averages are calculated for each year's summer (mobile ice) and winter (landfast ice) season defined by an ice index (gray step function). Note large variations in seasonally averaged freshwater flux and more uniform volume flux averages.

Our 2007-09 mooring data document changing freshwater flux to the west of Greenland. These Canadian International Polar Year data were recovered in August of 2009 and are available to us (see letter by Dr. Melling). The 2007-09 data require careful processing along the lines discussed by Münchow and Melling (2008) and Rabe et al. (2010).

We here propose a comprehensive and uniform data analysis of the entire 2003-09 data set using correlation and pattern analyses in time/frequency as well as in vertical space/wavenumber and lateral spatial domains. We will focus on vertical current shear and density stratification within the section. Figure 3 shows two preliminary snapshots of extreme along-channel velocity. Time series of volume flux derived from these, also presented, provide temporal context. The dynamical framework to be discussed next will guide analysis interpretations.

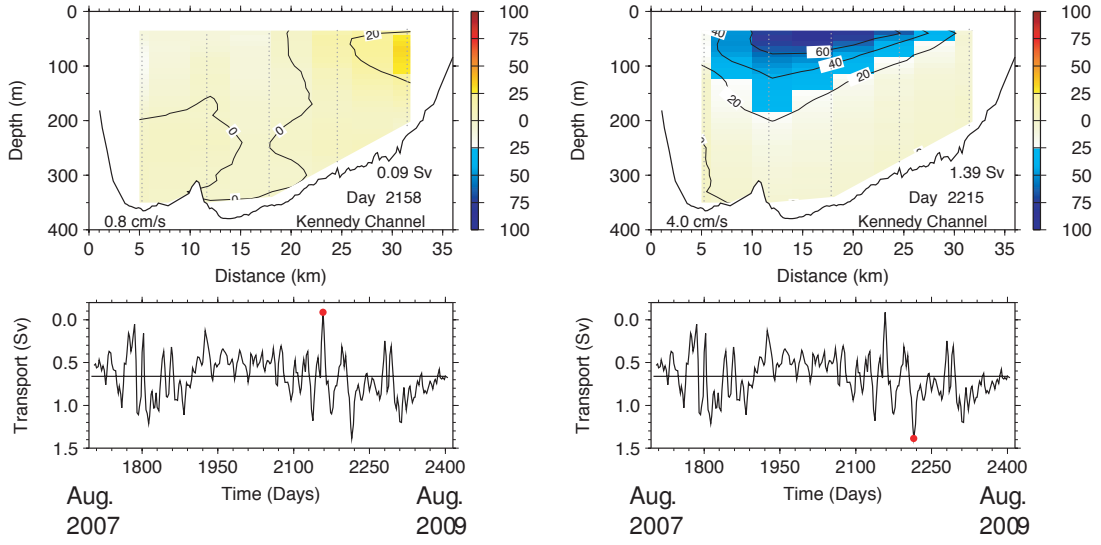

Figure 3: Two snapshots of low-pass filtered along-channel velocity section from 2007-09 ADCP mooring array (top panels) and time series of volume flux (bottom panel) with symbol indicating the time (days after Jan.-1, 2003) and transport for which the section is shown. View is to the north, Greenland on the right, and negative (blue) velocity contours indicate flow to the south.

3.2 Dynamical Framework

Valle-Levinson (2008) presents analytical model results that categorize idealized buoyant discharge problems with two non-dimensional parameters, i. e. the ratio between the channel width and the internal Rossby radius of deformation (Kelvin number, measure of baroclinic pressure gradients) and the ratio between the vertical boundary layer thickness and the channel depth (Ekman number, measure of friction). The linear, steady-state momentum balances along and across a density stratified channel with variable bottom depth consist of Coriolis acceleration, barotropic and baroclinic pressure gradients due to sloping sea surface and density surfaces, and vertical friction:

$$-fv = -g\frac{\partial \eta}{\partial x} + \frac{g}{\rho}\frac{\partial \rho}{\partial x}z + A_z\frac{\partial^2 u}{\partial x^2} \tag{1}$$

$$fu = -g\frac{\partial \eta}{\partial y} + \frac{g}{\rho}\frac{\partial \rho}{\partial y}z + A_z\frac{\partial^2 v}{\partial x^2} \tag{2}$$

A Kelvin number is defined as $K_e = W/L_D$, where W is the channel width and L_D is the internal Rossby radius ($L_D = \sqrt{g\,\Delta\rho\,D/\rho_0}\,/f$ with g the gravitational constant, $\Delta\rho$ the density anomaly, D a vertical scale of motion, ρ_0 the mean density, and f the Coriolis parameter) (Garvine, 1995). In the model the across-channel pressure gradients are prescribed to decay exponentially with spatial scale L_D. Surveys of Nares Strait indeed suggest such across-channel pressure gradients supporting the exponential decay with $L_D \sim 10$ km which gives a $K_e \sim 4$ (Münchow et al., 2006).

The second parameter, the Ekman number E_k, describes the vertical friction term and is given by $E_k = D_E^2/H^2$ for frictional boundary layer depth $D_E = \sqrt{A_z/f}$ with vertical viscosity A_z and H the local water depth. Typical Ekman layer scales are about 30 m in 300 m deep Nares Strait. We thus expect $E_k \sim 0.01$. However, we will need to modify the model in two ways. First, we will prescribe a non-zero volume flux, unlike Valle-Levinson (2008) and second, more importantly, the seasonal ice cover in Nares Strait changes the surface boundary condition from no-stress to no-slip when the ice is landfast.

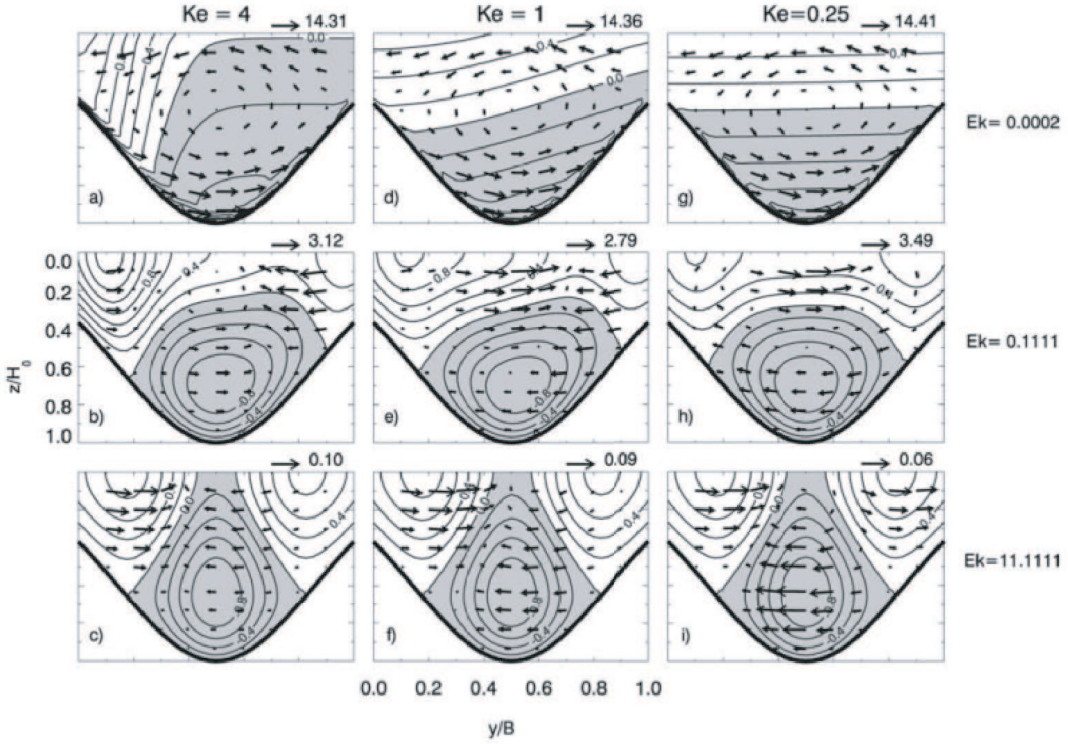

Figure 4: Model predictions of along and across-channel flows for six different model setting as the width decreases from 4 to 0.25 times the internal Rossby radius (left to right) and bottom friction increasing from top to bottom. Vertical and across-channel variables are non-dimensionalized with the bottom depth at the channel center H and the channel width W, respectively. The view is to the north with shading indicating northward flow and white contours indicating buoyant southward flow for a zero total volume flux (Valle-Levinson, 2008).

The model neglects non-linear advection, which is characterized by a third parameter of stratified flows, the internal Froude number $F_r = (U/f)/L_D$, where U is an along-shore velocity scale. Using values for Nares Strait (Münchow and Melling, 2008), we estimate $F_r \sim 0.1$. The Rossby number $R_o = F_r/K_e \sim 0.025 \ll 1$ scales non-linear advection, which thus is indeed negligible in our context as stated in equations (1) and (2).

Figure 4 shows model predictions for 6 different parameter settings (E_k, K_e) for a given channel. Note the dramatically different circulations from the ($K_e = 4, E_k = 0.0002$) to the

($K_e = 1, E_k = 0.11$) setting. This is the range of the parameter space that we expect to find Nares Strait. Kelvin, Ekman, and Rossby (or Froude) numbers for Nares Strait are similar to those of the Norwegian (Mork, 1981) and Delaware Coastal Currents (Münchow and Garvine, 1993) where density stratification affects much of the water depth, rotational and frictional effects are important, and non-linear advection is negligible.

4 Approaches

Using extensive mooring and satellite data from 2003 through 2009 and an idealized modeling component, we will investigate the dynamics separately for distinct dynamical regimes that we define as (a) the landfast ice season that we refer to as winter, (b) the mobile ice season that we call summer, and (c) the transition between these. Note that this definition of dynamical regimes does not correspond to calendar seasons, as our observational period includes two years without a "winter", namely 2006/07 and 2008/09. We will also analyze the characteristics of these regimes with regard to freshwater flux (e.g., Figure 2), their forcing functions, and potential predictability based on limited data accessible in real time from, e.g., new Canadian and Danish weather stations deployed in 2008 and 2009 within Nares Strait as well as a permanent tide gauge at Alert.

4.1 Ocean Current and Density Fields

Tides The flow in Nares Strait is dominated by mixed diurnal and semi-diurnal tidal currents (Figure 5) that agree well with barotropic model predictions (Padman and Erofeeva, 2004). More than 93% of the kinetic energy resides at tidal frequencies (Münchow and Melling, 2008). Barotropic tidal currents, as indicated by the small variations of current phase and orientation (not shown) do not, however, imply vertically uniform tidal currents, because friction introduces enhanced shears near vertical (and perhaps lateral) boundaries. For the 2003-06 observational period we find an almost linear current profile of M_2 tidal current amplitudes throughout most of the water column adjacent to the Ellesmere coast (Figure 5B, KS02, black symbols). This contrasts with the more logarithmic current profile in the center of the channel (Figure 5B, KS10, red symbols). These different frictional boundary layer structures allow dynamical investigations to reveal different dynamics and vertical eddy viscosity profiles (Prandle, 1982). We here propose such an investigation using harmonic analyses (Münchow et al., 1992) with vertical function fitting (Münchow et al., 2007). The best fits will suggest eddy viscosities that may differ for semi-diurnal and diurnal tidal constituents. Eddy viscosities for the the subinertial diurnal motions may also apply to low frequency synoptic variability.

Vertical profiles of tidal properties may also vary depending on the type of ice cover. Hence we will conduct analyses separately for land-fast (winter) and mobile (summer) ice conditions. We expect surface and bottom boundary layers to differ on account of

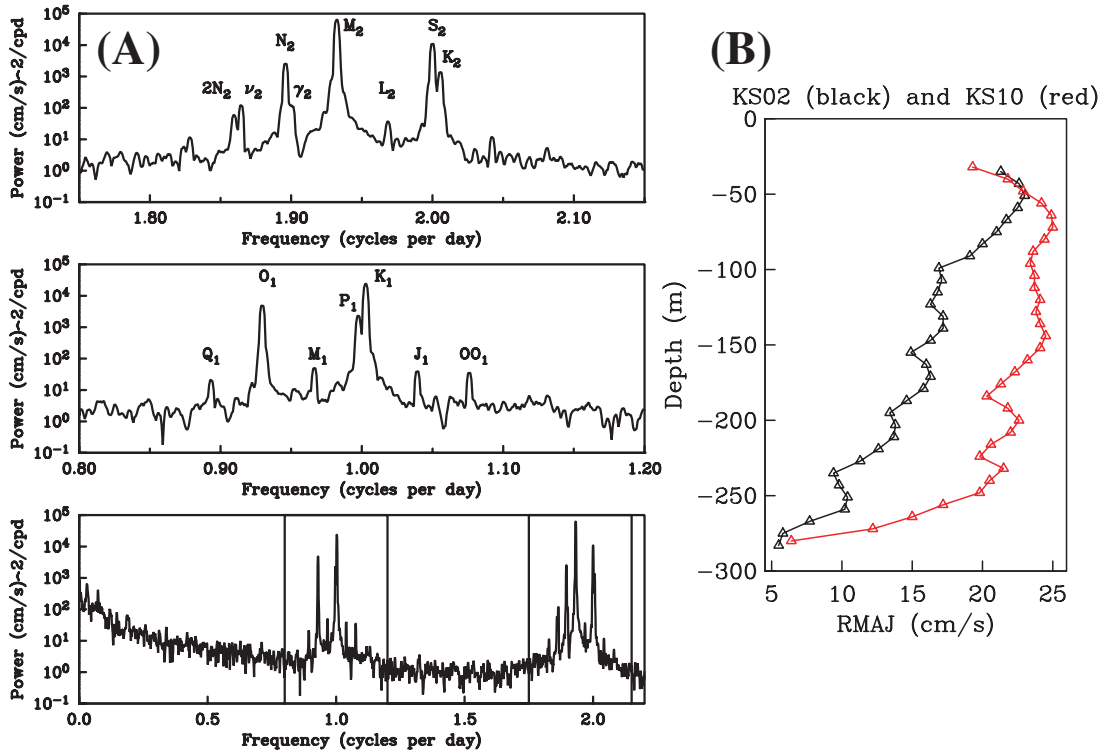

Figure 5: (A) Power spectra of vertically averaged along-channel currents at mooring KS10 for semi-diurnal (top), diurnal (middle), and 0-2.2 cycles per day (bottom) frequency bands (Münchow and Melling, 2008). (B) Vertical profiles of M_2 tidal current amplitude in the center of the channel (KS10, red) and adjacent to Ellesmere Island (KS02, black). Data are from 2003-06.

different surface roughness elements in the form of ice keels at the surface and small pebbles and silt at the bottom.

Subinertial Scales The multiple large spectral peaks at tidal frequencies seen in Figure 5 imply strong forth-nightly, monthly, and annual modulations of tidal current intensities. These cause enhanced vertical mixing of properties and momentum relevant for motions at subtidal frequencies longer than about a day. Spectral analyses of vertically averaged currents suggest enhanced variance at 10-day and 30-day scales at all measurement locations (Münchow and Melling, 2008), but neither the forcing nor the vertical structure of the motions at these time scales have been investigated yet, although we suspect that both friction and along-channel pressure gradients both contribute to their dynamics.

We thus propose to use both 2003-06 and 2007-09 data to investigate how variance is distributed vertically and how this distribution varies as the ice cover changes from landfast to mobile and vice versa. We will conduct separate frequency domain analyses for these two different dynamic regimes (winter vs. summer) to determine what forces the observed stratified flows. How important are the local winds in driving circulation? Do along-channel pressure gradients oppose or enhance the wind-driven flows? How deep

in the vertical does the wind forcing penetrate the water column adjacent to the Ellesmere and Greenland coasts and in the channel center? How deep does the frictional retardation of surface flow extend during the landfast ice winter season? Can we extract across-channel secondary circulation that appears prominently in mid-latitude observations and in steady-state linear model predictions such as Figure 4?

In order to address these questions, we require spatially and temporally coherent density and velocity fields, but unfortunately, the 2003-06 velocity data reveal low spatial coherence across the section, because of 3 failed instrument recoveries in 2006. In contrast, the recovered 2007-09 data are without any gaps in time or space and thus will reveal lateral scales, patterns, and coherence more fully. We thus propose to use these velocity data to find dominant spatially coherent flow field patterns via frequency domain empirical orthogonal function analyses, which allows description of both standing and propagating current patterns. We will correlate the temporal modulations of these spatial patterns with forcing functions such as pressure gradients, local winds, and frictional forces.

Despite less than ideal ADCP velocity records for the 2003-06 period, the data describing the density fields are resolved very well by six recovered CT/D (conductivity, temperature, and pressure) moorings (Rabe et al., 2010). At two locations we compare measured vertical current shear from the ADCP with estimated geostrophic shear from the CT/D moorings. The agreement in the center of the channel is good, as about 60% of the variance is correlated with a regression coefficient (gain) close to 1 at periodicities longer than 5 days. However, the agreement is poor at adjacent to the Ellesmere Island at KS02 coast where with a gain between ADCP and geostrophic velocities reaches 2 (Rabe, Ph.D. dissertation, in prep.). Hence the observed currents from the ADCP at KS02 are a factor of two smaller than the geostrophic currents estimated from CT/D data. Figure 4 suggests a possible explanation for $K_e = 4$. Velocities increase continuously towards the coast for the almost inviscid case $E_k = 0.0002$ that resembles our geostrophic estimates. In contrast, the more viscous case $E_k = 0.11$ results in a jet with largest velocities seaward that more closely resembles our directly measured ADCP velocities. Note that the model excludes lateral friction which warrants closer examination also.

Interannual Scales The 2003-06 time series of salinity and velocity contain significant linear trends indicating temporal variability at scales longer than 3 years. Figure 6B shows an example that reflects change in the spatial distribution of density. The baroclinic component of the geostrophic velocity field indicates the transition of a flow field consisting of a single jet in the center of the channel in 2003 to a flow field with a diminished jet in the center channel and an emerging coastal current adjacent to Ellesmere Island in 2006. The volume flux for these velocity sections is similar to within better than 10% of the 0.5 Sv (Figure 2), but what causes the development of a density field that suggest two separated southward flows where initially there was only one? Do these trends continue for the 2007-09 periods? Is this interannual evolution of the density field a pre-cursor to the failure of a southern ice arch to form in 2006/07 and again in 2008/09? The answers to such questions address the posed hypotheses.

Ocean Flux The flux F is a function of the velocity $U(y, z, t)$ perpendicular to a section of

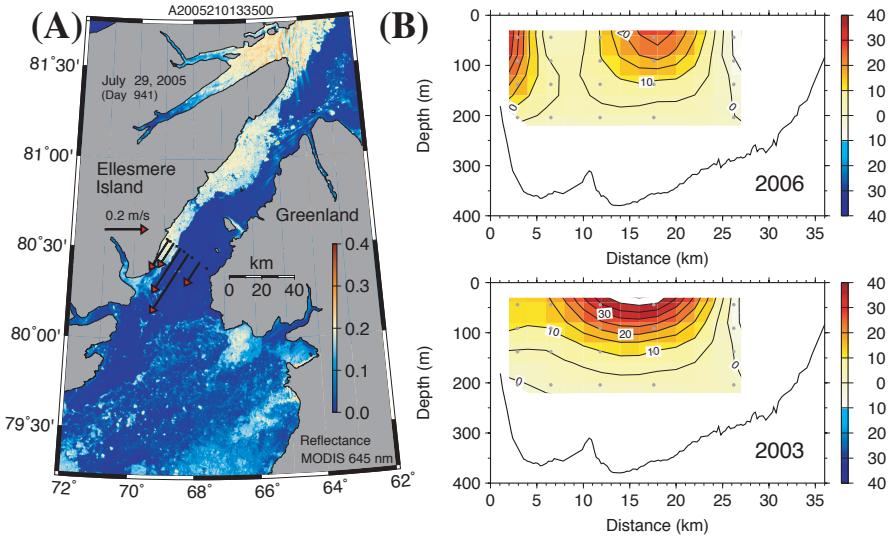

Figure 6: (A) Snapshot of surface reflectance at 250-m resolution in a visible band of MODIS-Aqua. Colors represent ice (yellow) and water (blue) for 29 July 2005 during a strong buoyant discharge event. Overlaid are vectors of geostrophic velocity in top layers estimated from 6 CT/D moorings across the section (Rabe et al., 2010). (B) Geostrophic velocities estimated for 2003 and 2006 from a linear trend analysis. The view is to the north, Greenland is on the right, and positive velocity contours (red) indicate flow to the south.

area $A = \int\int dy\, dz$ and a property $\phi(y,z,t)$, that is, $F = \int_A u\phi\, dA$. For the volume flux $\phi = 1$, while for freshwater flux $\phi = (S_0 - S(y,z,t))/S_0$ for a reference salinity S_0. The observed freshwater flux is the weighted sum of discrete velocity observations, where the weights are spatially variable salinity anomalies. The salinity anomalies are largest near the surface as the freshest waters always reside there. Melling (2000) reviews freshwater flux estimates from data in the Canadian Archipelago (Prinsenberg and Bennett, 1987) and finds that up to 50% of the flux in summer (winter) occurs in the upper 10 m (44 m).

Measurements are notoriously difficult to obtain in ice-covered water within a ∼30 m thick surface boundary layer that neither bottom-mounted ADCP nor subsurface CT/D moorings penetrate. This boundary layer is almost certainly influenced by frictional stresses at the ice-water (land-fast ice) or water-air (mobile ice) interface. Both salinity and velocity observations need to be extrapolated into this layer for reliable freshwater flux estimates. We here propose to apply a modified version of Münchow et al. (2007) to extrapolated velocity observations from below 30 m depth to the surface assuming an Ekman layer profile overlaid with a constant shear, i.e.,

$$u(z) = u_0 + u_1\, z + v_E\, s(z) + u_E\, c(z) \tag{3}$$

$$v(z) = v_0 + v_1\, z + v_E\, c(z) - u_E\, s(z) \tag{4}$$

where z is the vertical distance from the surface scaled by the vertical Ekman layer depth D_E (defined in section 3.2) while $s(z) = \sin(z)\, e^z$ and $c(z) = \cos(z)\, e^z$ are the functions

to describe the Ekman layer profile. The 6 free parameters (u_0, v_0), (u_1, v_1), and (u_E, v_E) are determined by minimizing the squared differences from velocity profiles. Note that the along- and across-channel velocity components are fitted concurrently. The degrees of freedom thus are 2N-6 where N is the number of vertical velocity measurements used in the fit. We will modify the procedure during the land-fast ice winter by prescribing a zero velocity at the ice-water interface and during the mobile ice summer by using estimates from satellite (section 4.2) and modeling (section 4.3) analyses of surface velocities. Available ice-profiling sonar measurements at two locations within our section will also be used. Preliminary inspection of these data indicate that ice thicker than 10 m is not uncommon and floes with average thickness of 30 m passed over our moorings on Oct. 25, 2006 (Melling, 2007). MODIS motion vectors may provide a complementary, albeit a less certain, constraint on a surface velocity estimate.

4.2 MODIS Satellite Imagery

Recently, we have begun quantitative analysis of satellite imagery for Nares Strait. Following Luo et al. (2008), Trishchenko et al. (2009), and Wang and Shi (2009), we convert raw level-0 MODIS satellite retrievals via processing, calibration, re-projection, and gridding to level-1B data to preserve high spatial resolutions. We use only open public domain sources and software that we document and distribute at
http://muenchow.cms.udel.edu/html/RemoteSensing.

This approach ensures complete control of digital data in engineering units to retain the nominal 250 m and 500 m spatial resolution at nadir for the relevant seven optical and near-infrared frequency bands. This flexible and efficient access to digital engineering data is essential for quantitative, as opposed to qualitative, scientific analyses. As an example of the type of analyses we envision, we show in Figure 7 preliminary results of motion vectors derived from a sequence of 6 MODIS-Terra scenes for a 23-hour period August 8/9, 2009, near our mooring section in Nares Strait. We derive these vectors from standard lagged cross-correlation analyses of two sequential scenes loosely following ideas presented and applied by Kwok et al. (1998) to ice motion and Cayula and Cornillon (1995) to temperature fronts. We are still experimenting with optimal settings for Nares Strait and the adjacent Lincoln Sea to the north, but Figure 7 was derived for features with scales of 1 km. We have developed an algorithm to distinguish between pixels containing water, clouds, and ice categories using ratios between reflectance at different high resolution MODIS bands (Luo et al., 2008). We here propose to fully implement these to track ice as opposed to ill-defined "features." Nevertheless, cautiously interpreting Figure 7, a generally southward flow emerges with much enhanced velocities near the Ellesmere Island coast. Additionally, however, we find areas of convergence and divergence near islands and coastal capes (Wolfe and Cenedese, 2006).

The proposed effort includes fully developing these capabilities within a larger analysis of all available 2003-09 Nares Strait data. For example, we will verify ice motions over the mooring section with ocean observations and the ice model described below.

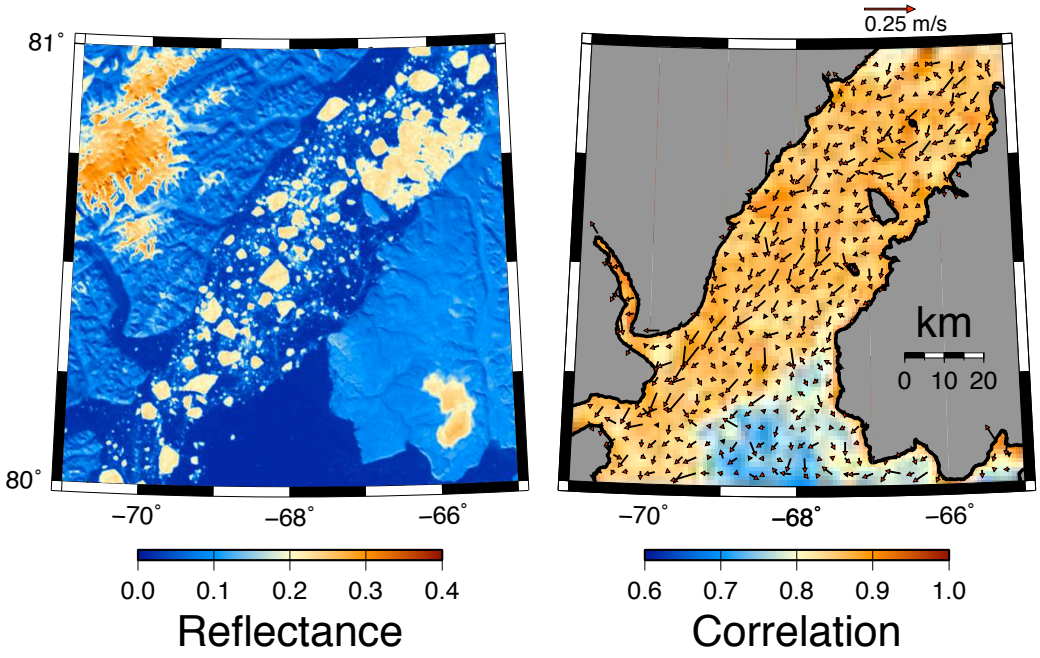

Figure 7: Snapshot of subtidal motion vectors for Aug. 8/9, 2009 derived from six MODIS-Terra images for a 23-hour period (right) and the reflectance for Aug. 8, 2009, 17:30 UTC (left). Color in the right panel indicate average correlations between images used to derive the velocities.

More specifically, the (ice) surface backscatter sensed by our bottom mounted ADCPs can be used under special circumstances to estimate an ice velocity (Melling, pers. comm., 2009). We will estimate error fields independently by using motion vectors over land.

Note that the high temporal resolution of MODIS in our study area during the summer, with 6-14 largely cloud-free scenes, resolves tidal currents that less frequent, but more reliably satellite radar data retrievals from RADARSAT and ENVISAT-ASAR do not. Our approach, while limited to cloud-free optical data generally available during the summer season only, thus reduces the substantial tidal biases that would occur in Nares Strait. Hence we are confident to estimate ice flux during the summer season from a combination of MODIS scene analysis (ice velocity), moored 2003-09 ice-profiling sonar data (ice thickness at two locations on the section), and the ice model.

4.3 Ice Thickness, Flux, and Modeling

The data set we have collected contains a unique combination of ocean velocity measurements and ice thickness data derived from upward-looking sonar (Fissel et al., 2008; Melling, 1998). Adding to these the satellite analysis described above, we provide an observational basis with which to study the physics of ice motion. The ice modeling component will supplement the data to address open questions of surface velocities and stress at the ice-ocean interface. One obstacle for estimating the total freshwater flux through

Nares Strait is the lack of velocity measurements in the upper 30 m of the water column. Using the ice model to relate independent observations of ice thickness and ice velocities to oceanic stresses permits the estimation of an ocean surface velocity. An interpolation between the surface and the 30-m depth is then possible using Ekman theory as used in Münchow et al. (2007) for vessel-mounted ADCP surveys (see section 4.1 on Ocean Flux).

We propose to investigate the ice physics responsible for the observed patterns of ice thickness (moored upward-looking sonar data), ice concentration, and ice motion (from MODIS imagery) within a simple dynamical framework. The momentum equation for ice can be taken as

$$m\frac{\partial \mathbf{u}}{\partial t} + m(\mathbf{u}\cdot\nabla)\mathbf{u} = \tau_a + \tau_o - mf\hat{k}\mathbf{u} - mg\nabla H + \nabla\cdot\sigma, \tag{5}$$

where m is the mass, $\mathbf{u}$ is the ice velocity, τ_a and τ_o are the atmospheric and oceanic stresses, respectively, f is the Coriolis parameter, g the gravitational constant, ∇H the sea surface tilt, and σ the internal stress. The observations provide an estimate of m and $\mathbf{u}$. The internal stress is a complicated function of the imposed forces and the ice properties, primarily thickness and concentration, which is generally derived from the particular ice rheology chosen for an ice model. Our goal here is to extract an estimate of τ_o by employing an ice model implementing equation (5).

For the ice model, we will use the CICE model developed at Los Alamos (Hunke and Lipscomb, 2008). It has both a dynamic and a thermodynamic component, permits either prescribed boundary forcing or coupling to ocean and/or atmospheric models, and incorporates state-of-the-art physical parameterizations. Feltham (2008) and Morales Maqueda et al. (2004) provide modern reviews of ice rheology and polynyas from theoretical and observational perspectives that place CICE into a general context. CICE relies on the elastic-viscous-plastic (EVP) rheology from Hunke and Dukowicz (1997), which is a variation of the rheology developed by Hibler (1979), who postulated nonlinear viscous-plastic behavior, with an elliptic yield curve that incorporates zero resistance to pure tension and cohesion under moderate shear. The appeal of this particular rheology for our purposes, in addition to its widespread use in a variety of contexts throughout the literature, is that it has been applied successfully to the problem of modeling ice arches (Dumont et al., 2009). In our study area, ice arch formation and collapse determines the timing and subsequent evolution of land-fast ice and mobile ice.

In the EVP rheology, ice strength enters in two variables, the ellipticity e for the ratio of shear to normal strength and P for normal strength. e can be freely assigned in the model and is typically held constant throughout one simulation. CICE allows for two different definitions of the compressive strength P, one following Hibler (1979), the other relating the ice strength to the redistribution of potential energy through ridging. Hunke and Lipscomb (2008) find that the latter formulation is more physically realistic but also more prone to numerical instability. We plan to work mostly with Hiblers parameterization $P = P^* h e^{[-A(1-c)]}$, where P^* and A are empirical constants, set to 27,500 N/m and 20, respectively; h is the mean ice thickness; and c is the ice concentration. Aside from

the numerical issues, it has the added benefit of exhibiting more clearly the relationship between ice strength and the ice properties of thickness and concentration. Moreover, it is the formulation used in previous ice arch studies (Dumont et al., 2009).

For our purposes, we will restrict our investigation to an idealized funnel-shaped channel, with uniform width and converging and diverging openings at its northern and southern termini. The wind forcing will be prescribed based on past observations and atmospheric modeling results. Our goals are (1) an exploratory parameter study, primarily concerning the ice rheology (e) and prescribed wind stress, to focus our investigation on a regime consistent with the data, (2) first estimates for along-channel ice motion vectors to interpolate in time when no MODIS motion vectors are available, (3) using a blend of MODIS and CICE velocities, along with ice thickness observations, to determine an ocean surface velocity estimate, and (4) to interpolate between the ocean surface velocity estimate and ADCP velocity observations terminating at $\sim$ 30 m depth with weighted least squares function fitting (Equations 3 and 4). We emphasize that we are not attempting to couple our ice model directly to either atmospheric or ocean models as does the companion proposal submitted by Dr. Samelson.

5 Broader Impacts

Education The education of students and teachers to critically evaluate physical and statistical methods, data, and analyses is much needed to improve both public and scientific debate related to climate change. The proposed effort will support two female first-year Ph.D students, Patricia Ryan and Jamie Shutta, in addition to two undergraduate and two local science teachers to work together as summer interns. The PIs, one of whom (Helga Huntley) is a first-time female investigator, will facilitate daily summer workshops to train students and teachers on transferable research skills focused on (but not limited to) the MODIS real-time satellite retrieval, processing, analyses, and interpretations of evolving ice motion fields.

International science planing This proposal contributes substantially to US participation, continuity, and data dissemination within an ongoing, informal, international, collaborative effort of a "Friends of Nares Strait" group that includes young and old researchers from Denmark, Scotland, England, Canada, and the USA.

Services Both Canadian, Danish, and US government agencies and private service providers frequently rely on our data and expertise in order to aid their clients. This includes companies with interests in oil fields on the continental shelf off Labrador, US Naval officers charged with operational ice prediction, Canadian icebreaking operations, as well as authorities in Greenland charged with natural resource management.

References

Aagaard, K. and E. C. Carmack, 1989: The role of sea ice and other fresh-water in the Arctic circulation. *J. Geophys. Res.*, **94(C10)**, 14485–14498.

Alkire, M. B., K. K. Falkner, I. Rigor, M. Steele, and J. Morison, 2007: The return of Pacific waters to the upper layers of the central Arctic Ocean. *Deep-Sea Res.*, **54(9)**, 1509–1529.

Belkin, I. M., 2004: Propagation of the "Great Salinity Anomaly" of the 1990s around the northern North Atlantic. *Geophys. Res. Let.*, **31(8)**, L08306.

Bryden, H. L., H. R. Longworth, and S. A. Cunningham, 2005: Slowing of the Atlantic meridional overturning circulation at 25 degrees N. *Nature*, **438(7068)**, 655–657.

Cayula, J. and P. Cornillon, 1995: Multi-image edge detection for SST images. *J. Atmos. Oceanic Technol.*, **12(4)**, 821–829.

Copland, L., D. R. Mueller, and L. Weir, 2007: Rapid loss of the Ayles ice shelf, Ellesmere Island, Canada. *Geophys. Res. Let.*, **34(21)**, L21501.

Curry, R. and C. Mauritzen, 2005: Dilution of the northern North Atlantic Ocean in recent decades. *Science*, **308(5729)**, 1772–1774.

Dickson, B., I. Yashayaev, J. Meincke, B. Turrell, S. Dye, and J. Holfort, 2002: Rapid freshening of the deep North Atlantic Ocean over the past four decades. *Nature*, **416(6883)**, 832–837.

Dickson, R., B. Rudels, S. Dye, M. Karcher, J. Meincke, and I. Yashayaev, 2007: Current estimates of freshwater flux through Arctiac and subarctic seas. *Progr. Oceanogr.*, **73(3-4)**, 210–230.

Dumont, D., Y. Gratton, and T. E. Arbetter, 2009: Modeling the dynamics of the North Water polynya ice bridge. *J. Phys. Oceanogr.*, **39(6)**, 1448–1461.

Emile-Geay, J., M. A. Cane, N. Naik, R. Seager, A. C. Clement, and A. van Geen, 2003: Warren revisited: Atmospheric freshwater fluxes and "why is no deep water formed in the North Pacific". *J. Geophys. Res.*, **108(C6)**, 3178.

Falkner, K. K., M. OBrian, H. Melling, E. Carmack, A. Münchow, and E. Jones, 2009: Interannual variability of dissolved nutrients in the Canadian Archipelago and Baffin Bay with implications for freshwater flux. *J. Geophys. Res.*, **submitted**, 55pp.

Feltham, D. L., 2008: Sea ice rheology. *Ann. Rev. Fluid Mech.*, **40**, 91–112.

Fissel, D. B., J. R. Marko, and H. Melling, 2008: Advances in upward looking sonar technology for studying the processes of change in Arctic Ocean ice climate. *J. Operat. Oceanogr.*, **1(1)**, 9–18.

Garrett, C., 2004: Frictional processes in straits. *Deep-Sea Res. part II*, **51(4-5)**, 393–410.

Garvine, R. W., 1995: A dynamical system for classifying buoyant coastal discharges. *Cont. Shelf Res.*, **15(13)**, 1585–1596.

Hibler, W. D., 1979: Dynamic thermodynamic sea ice model. *J. Phys. Oceanogr.*, **9**, 815–846.

Holland, M. M., J. Finnis, A. P. Barrett, and M. C. Serreze, 2007: Projected changes in Arctic Ocean freshwater budgets. *J. Geophys. Res.*, **112(G4)**, G04S55.

Hunke, E. and W. Lipscomb, 2008: Cice: the los alamos sea ice model documentation and software user's manual version 4.0. *Los Alamos National Laboratory Tech. Rep. LA-CC-06-012*, 52 pp.

Hunke, E. C. and J. K. Dukowicz, 1997: An elastic-viscous-plastic model for sea ice dynamics. *J. Phys. Oceanogr.*, **27**, 1849–1867.

Hurrell, J. W. and C. Deser, 2009: North Atlantic climate variability: The role of the North Atlantic Oscillation. *J. Mar. Sys.*, **78(1)**, 28 – 41.

Johnson, H. L. and C. Garrett, 2006: What fraction of a Kelvin wave incident on a narrow strait is transmitted? *J. Phys. Oceanogr.*, **36(5)**, 945–954.

Khatiwala, S. P., R. G. Fairbanks, and R. W. Houghton, 1999: Freshwater sources to the coastal ocean off northeastern North America: Evidence from (h2o)-o-18/(h2o)-o-16. *J. Geophys. Res.*, **104(C8)**, 18241–18255.

Koenigk, T., U. Mikolajewicz, H. Haak, and J. Jungclaus, 2007: Arctic freshwater export in the 20th and 21st centuries. *J. Geophys. Res.*, **112(G4)**, G04S41.

Kwok, R., A. Schweiger, D. Rothrock, S. Pang, and C. Kottmeier, 1998: Sea ice motion from satellite passive microwave imagery assessed with ERS SAR and buoy motions. *J. Geophys. Res.*, **103(C4)**, 8191–8214.

Lindsay, R. W., J. Zhang, A. Schweiger, M. Steele, and H. Stern, 2009: Arctic sea ice retreat in 2007 follows thinning trend. *J. Clim.*, **22(1)**, 165–176.

Luo, Y., A. P. Trishchenko, and K. V. Khlopenkov, 2008: Developing clear-sky, cloud and cloud shadow mask for producing clear-sky composites at 250-meter spatial resolution for the seven MODIS land bands over Canada and North America. *Remote Sens. Env.*, **112(12)**, 4167–4185.

Melling, H., 1998: Sound scattering from sea ice: Aspects relevant to ice-draft profiling by sonar. *J. Atmos. Oceanic Technol.*, **15(4)**, 1023–1034.

—, 2000: *Exchange of freshwater transport through the sahllow straits of the North American Arctic*, Kluwer Academic Publishers, Dordrecht, Netherlands, chap. 20. pp. 479–502.

—, 2007: Canadian Arctic Through-Flow 2007 cruise to Nares Strait. CCGS Henry Larsen, August 9 – September 1, 2007, Institute of Ocean Sciences Cruise 2007-52, available at http://muenchow.cms.udel.edu/Reports/Larsen2007ScienceReport.pdf, 33pp, unpublished.

Melling, H., T. Agnew, K. Falkner, D. Greenberg, C. Lee, A. Münchow, B. Petri, S. Prinsenberg, R. Samelson, and R. Woodgate, 2008: *Fresh-water fluxes via Pacific and Arctic outflows across the Canadian polar shelf*, Springer Verlag, Dordrecht, Netherlands, chap. 9. pp. 193–261.

Melling, H., Y. Gratton, and G. Ingram, 2001: Ocean circulation within the North Water polynya of Baffin Bay. *Atmos.-Oceans*, **39(3)**, 301–325.

Morales Maqueda, M. A., A. J. Willmott, and N. R. T. Biggs, 2004: Polynya dynamics: A review of observations and modeling. *Rev. Geophys.*, **42(1)**, RG1004.

Morison, J., M. Steele, and R. Andersen, 1998: Hydrography of the upper Arctic Ocean measured from the nuclear submarine USS Pargo. *Deep-Sea Res.*, **45(1)**, 15–38.

Mork, M., 1981: Circulation phenomena and frontal dynamics of the Norwegian Coastal Current. *Phil. T. R. Soc. A*, **302(1472)**, 635–647.

Münchow, A., K. Falkner, and H. Melling, 2007: Spatial continuity of measured seawater and tracer fluxes through Nares Strait, a dynamically wide channel bordering the Canadian Archipelago. *J. Mar. Res.*, **65 (6)**, 759–788.

Münchow, A. and R. W. Garvine, 1993: Dynamical properties of a buoyancy-driven coastal current. *J. Geophys. Res.*, **98(C11)**, 20063–20077.

Münchow, A., A. K. Masse, and R. W. Garvine, 1992: Astronomical and nonlinear tidal currents in a coupled estuary shelf system. *Cont. Shelf Res.*, **12(4)**, 471–498.

Münchow, A. and H. Melling, 2008: Ocean current observations from Nares Strait to the west of Greenland: Interannual to tidal variability and forcing. *J. Mar. Res.*, **66 (6)**, 801–833.

Münchow, A., H. Melling, and K. K. Falkner, 2006: An observational estimate of volume and freshwater flux leaving the Arctic Ocean through Nares Strait. *J. Phys. Oceanogr.*, **36(11)**, 2025–2041.

Myers, P. G., 2005: Impact of freshwater from the Canadian Arctic Archipelago on Labrador Sea Water formation. *Geophys. Res. Let.*, **32(6)**, L06605.

Padman, L. and S. Erofeeva, 2004: A barotropic inverse tidal model for the Arctic Ocean. *Geophys. Res. Let.*, **31(2)**, L02303.

Parkinson, C. L. and D. J. Cavalieri, 2008: Arctic sea ice variability and trends, 1979-2006. *J. Geophys. Res.*, **113(C7)**, C07003.

Peterson, B. J., R. M. Holmes, J. W. McClelland, C. J. Vorosmarty, R. B. Lammers, A. I. Shiklomanov, I. A. Shiklomanov, and S. Rahmstorf, 2002: Increasing river discharge to the Arctic Ocean. *Science*, **298(5601)**, 2171–2173.

Polyakov, I. V., V. A. Alexeev, G. I. Belchansky, I. A. Dmitrenko, V. V. Ivanov, S. A. Kirillov, A. A. Korablev, M. Steele, L. A. Timokhov, and I. Yashayaev, 2008: Arctic ocean freshwater changes over the past 100 years and their causes. *J. Clim.*, **21(2)**, 364–384.

Prandle, D., 1982: The vertical structure of tidal currents and other oscillatory flows. *Cont. Shelf Res.*, **1(2)**, 191–207.

Prinsenberg, S. J. and E. B. Bennett, 1987: Mixing and transports in Barrow Strait, the central part of the Northwest Passage. *Cont. Shelf Res.*, **7(8)**, 913–935.

Prinsenberg, S. J. and J. Hamilton, 2005: Monitoring the volume, freshwater and heat fluxes passing through Lancaster Sound in the Canadian Arctic Archipelago. *Atmos.-Oceans*, **43(1)**, 1–22.

Proshutinsky, A., R. Krishfield, M. L. Timmermans, J. Toole, E. Carmack, F. McLaughlin, W. J. Williams, S. Zimmermann, M. Itoh, and K. Shimada, 2009: Beaufort Gyre freshwater reservoir: State and variability from observations. *J. Geophys. Res.*, **114**, C00A10.

Rabe, B., A. Münchow, H. Johnson, and H. Melling, 2010: Nares Strait hydrography and salinity field from a three-year moored array. *J. Geophys. Res.*, **submitted Oct.-2009**, http://muenchow.cms.udel.edu/papers/RabeEtAl2009JGR.pdf.

Rignot, E. and K. Steffen, 2008: Channelized bottom melting and stability of floating ice shelves. *Geophys. Res. Let.*, **35(2)**, L02503.

Rigor, I. G., J. M. Wallace, and R. L. Colony, 2002: Response of sea ice to the Arctic oscillation. *J. Clim.*, **15(18)**, 2648–2663.

Sadler, H., 1976: Water, heat, and salt transport through Nares Strait, Ellesmere Island. *J. Fish. Res. Board Can.*, **33**, 2286–2295.

Samelson, R. and P. Babour, 2008: Low-level winds in Nares Strait: a model-based mesoscale climatology. *Mon. Weather Rev.*, **136**, 4746–4759.

Samelson, R. M., T. Agnew, H. Melling, and A. Münchow, 2006: Evidence for atmospheric control of sea-ice motion through Nares Strait. *Geophys. Res. Let.*, **33(2)**, L02506.

Serreze, M. C. and J. A. Francis, 2006: The Arctic amplification debate. *Clim. Change*, **76(3-4)**, 241–264.

Stacey, M. W., S. Pond, and P. H. LeBlond, 1991: Flow dynamics in the Strait of Georgia, British Columbia. *Atmos.-Ocean*, **29(1)**, 1–13.

Sundby, S. and K. Drinkwater, 2007: On the mechanisms behind salinity anomaly signals of the northern North Atlantic. *Progr. Oceanogr.*, **73(2)**, 190–202.

Toulany, B., B. Petrie, and C. Garrett, 1987: The frequency-dependent structure and dynamics of flow fluctuations in the Strait of Belle Isle. *J. Phys. Oceanogr.*, **17(2)**, 185–196.

Trishchenko, A. P., Y. Luo, K. V. Khlopenkov, W. M. Park, and S. Wang, 2009: Arctic circumpolar mosaic at 250 m spatial resolution for IPY by fusion of MODIS/TERRA land bands B1-B7. *Int. J. Remote Sens.*, **30(6)**, 1635–1641.

Valle-Levinson, A., 2008: Density-driven exchange flow in terms of the Kelvin and Ekman numbers. *J. Geophys. Res.*, **113(C4)**, C04001.

Wang, M. and W. Shi, 2009: Detection of ice and mixed ice-water pixels for modis ocean color data processing. *IEEE Trans. Geosci. Remote Sens.*, **47(8)**, 2510–2518.

White, D., L. Hinzman, L. Alessa, J. Cassano, M. Chambers, K. Falkner, J. Francis, W. J. Gutowski, M. Holland, R. M. Holmes, H. Huntington, D. Kane, A. Kliskey, C. Lee, J. McClelland, B. Peterson, T. S. Rupp, F. Straneo, M. Steele, R. Woodgate, D. Yang, K. Yoshikawa, and T. Zhang, 2007: The Arctic freshwater system: Changes and impacts. *J. Geophys. Res.*, **112(G4)**, G04S54.

Wolfe, C. L. and C. Cenedese, 2006: Laboratory experiments on eddy generation by a buoyant coastal current flowing over variable bathymetry. *J. Phys. Oceanogr.*, **36(3)**, 395–411.

Wunsch, C. and P. Heimbach, 2006: Estimated decadal changes in the North Atlantic meridional overturning circulation and heat flux 1993-2004. *J. Phys. Oceanogr.*, **36(11)**, 2012–2024.

Yang, J. Y., 2005: The Arctic and subarctic ocean flux of potential vorticity and the Arctic Ocean circulation. *J. Phys. Oceanogr.*, **35(12)**, 2387–2407.

Zweng, M. M. and A. Münchow, 2006: Warming and freshening of Baffin Bay, 1916-2003. *J. Geophys. Res.*, **111(C7)**, C07016.